Rheological and water transport properties of cement pastes modified with diutan gum and attapulgite/palygorskite nanoclays

Author 1 (Corresponding author):

Siwei Ma, Ph.D.

Columbia University, Department of Civil Engineering and Engineering Mechanics, 500 West 120th Street, New York, NY, 10027, USA

Tel.: +1 818 519 0736.

Email address: sm3614@columbia.edu

Author 2:

Shiho Kawashima, Associate professor and Ph. D.

Columbia University, Department of Civil Engineering and Engineering Mechanics, 500 West 120th Street, New York, NY, 10027, USA

Tel.: +1 212 854 2701.

Email address: sk2294@columbia.edu

Abstract

Viscosity modifying admixtures (VMAs) play a major role in achieving the desired rheological properties for 3D concrete printing. In addition to rheology, water transport properties are critically important – due to the absence of formwork, freshly printed components with high exposed surface areas are susceptible to excessive water loss. In this study, the effect of VMAs (i.e. attapulgite/palygorskite nanoclay and diutan gum) on water transport properties of cement pastes were investigated. Bleeding, water retention under suction pressure, and evaporation under air flow were measured. The nanoclay was found to reduce bleeding but had no effect on water retention or evaporation. The diutan gum was found to reduce bleeding, improve water retention, and decrease evaporation loss. The rheological properties of the pastes and their interstitial solution were also characterized to resolve the mechanisms underlying the water transport behaviors. Good correlation between the measured rheological parameters and water transport properties was found.

Keywords

Rheology; Bleeding; Evaporation; Water retention; Viscosity modifying admixtures

1. Introduction

Water transport property is the ability of water to move through the matrix of porous materials in response to a gradient of pressure. In concrete practice, water transport covers several different behaviors including bleeding, evaporation, and water loss from the fresh cement mixture into the substrate.

From the 1970s, water transport behavior has been recognized as a critical factor for successful building products, including render mortars, cementitious tile adhesives, and oil well cement slurries. In these applications, water movement in a fresh suspension can result from suction pressure from the substrate, usually described as "water retention." For instance, when stucco is applied on a substrate, such as bricks and plaster, water may be absorbed by the substrate; when oil well cement slurry is placed under pressure across a permeable rock formation, the water may be extracted by the rock formation (Desbrieres 1993). This phenomenon can induce insufficient hydration of cement. 3D concrete printing is an emerging construction technique that eliminates the need for formwork, which can expand aesthetic freedom but also reduce materials, labor, and time during construction (Lloret et al. 2015). However, for layer-based additive manufacturing, the freeform components exhibit relatively large exposed surface areas, which are susceptible to rapid evaporation of water. This can adversely affect material stability (i.e. the ability to stay homogeneous), hinder hydration and induce plastic shrinkage, ultimately impairing the eventual strength and durability of the printed structure. The surface moisture and bleeding rate of the fresh concrete are critical factors for the inter-layer strength of 3D printed elements (Sanjayan et al. 2018). Thus, this emerging technique requires a better understanding of water transport behavior.

Bleeding describes the phenomena when water rises or bleeds to the surface once the fresh concrete is placed. Free water escapes from cement particle flocs and flows out due to a density difference between the water and cement grains. (Perrot et al. 2012) summarized the criteria for the occurrence of bleeding. If colloidal attractive forces dominate gravity, there will be no bleeding. If gravity dominates colloidal attractive forces, bleeding occurs. The bleeding process is controlled by the viscosity of the interstitial solution and the permeability of the porous medium, in this case formed by cement particles, as illustrated by Darcy's law for a consolidation process, i.e. fluid flow through porous media (Ghourchian et al. 2016).

In most cases, bleeding is considered to be undesirable. Excessive bleeding weakens the bond between the cement matrix and the subsurface of aggregates, which induces a nonuniformity in strength (Mehta and Monteiro 2006). This has a major impact on the long-term durability of concrete. However, concrete mixtures with an inherent low rate of bleeding or low quantity of bleed water are susceptible to plastic shrinkage, which appears in concretes with large, exposed surface areas, such as decks, pavements, and floors. Sanjayan et al. (Sanjayan et al. 2018) demonstrated that moderate bleed water could be desirable in 3D concrete printing through improving surface moisture, which is the competition between bleeding and evaporation, thus increasing the inter-layer bond strength. Evaporation drying could be a major challenge for 3D concrete printing, which has no formwork to protect the material.

It is clear that controlling rheology will be key for 3D concrete printing. And viscosity modifying admixtures (VMAs) can be expected to play a major role in achieving the desired rheological properties for successful execution. VMAs can be classified as organic VMAs, such as starch and cellulose ether, and inorganic VMAs, such as clays and colloidal silicas. Khayat (Khayat 1998) reviewed and investigated the effect of polysaccharides as VMAs on cement-based systems. He also noted that due to the reduction of bleeding, concrete incorporating an organic VMA has an increased susceptibility to plastic shrinkage cracking. Generally speaking, the organic VMAs can improve water retention capacity (Brumaud et al. 2013; Bülichen et al. 2012; Khayat 1998; Patural et al. 2010a; Poinot et al. 2014). However, as a second generation organic VMA, the effect of diutan gum addition on the rheological and water transport properties are less studied. On the other hand, considering inorganic VMAs, nano-sized highly purified palygorskite clays can significantly increase the yield stress and shape stability of fresh cementitious materials (Kawashima et al. 2013a; Qian and Kawashima 2016; Quanji et al. 2014). Thus, these clays have been used for slip-form paving, reducing formwork pressure of self-consolidating concrete, and recently for the application of 3D concrete printing (Kazemian et al. 2017; Khoshnevis 2004; Kim et al. 2010; Voigt et al. 2010). However, to the authors' knowledge, no results have been reported on their water transport abilities.

The present work aims to evaluate the water transport behavior and rheological properties of cement pastes incorporating nanoclay and diutan gum through measurements of bleeding, water retention, water loss to evaporation and steady-state shear rheology.

2. Materials and Methods

2.1. Materials

The cement used was a Type I Portland cement and its chemical and mineralogical compositions are reported in Table 1. The Blaine fineness is 402 m^2/kg. Distilled water was used in all mixes.

Chemical Oxide	SiO_2	Al_2O_3	Fe_2O_3	CaO	MgO	SO_3	Loss on ignition
Cement (%)	19.27	4.68	3.51	63	3.21	2.72	2.09

Table 1. Chemical composition of Type I Portland Cement.

Two VMAs were investigated – a clay and a gum. A highly purified form of the mineral attapulgite, or palygorskite, was the clay chosen for the study. Attapulgite/palygorskite is a magnesium alumino silicate clay with the theoretical formula of $Si_8Mg_8O_{20}(OH)_2(H_2O)_4 \cdot 4H_2O$ (Galan 1996). The preferred name according to the International Nomenclature Committee is palygorskite, although the name attapulgite is better known commercially (Murray 1991). It is needle-like in structure – 1.75 μm in length and 30 nm in diameter (“ACTI-GEL® 208 - Acti-Gel” n.d.). Therefore, it can be referred to as a nanoclay. To disperse the nanoclay, it was blended with water in a Waring blender for 3 min to produce a suspension.

A commercially available diutan gum gel whose solid content is 1% by mass was the gum chosen for this study. Diutan gum is a polysaccharide produced by Sphingomonas bacteria in fermentation (Plank 2004). It has high molecular weight and anionic charges. It could bind positively charged cement particles to increase viscosity, which is utilized for various applications in the construction industry and the petroleum industry (Pei et al. 2015).

All cement pastes were prepared using a hand mixer at a speed of 540 rpm. Cement pastes with nanoclay were prepared by adding the cement to the nanoclay suspension, then mixing for 3 min. Cement pastes with diutan gum were prepared by adding cement to water, mixing for 1.5 min, adding diutan gum gel, then mixing for another 1.5 min. Thus, the pastes prepared with the nanoclay and the diutan gum both had a total paste mixing time of 3 min. Pastes were prepared with a water-to-cement (W/C) ratio of 0.34, 0.44 or 0.6, depending on the test.

2.2. Water transport measurements

2.2.1. Bleeding experiments

Just after mixing, pastes were poured into test tubes 29.4 mm in diameter and placed on a surface free of any vibration. After placement, the tube was sealed to prevent any water evaporation. The bleed water was then extracted with a pipet at 20 min intervals during the first 60 min, then at 60 min intervals for the remainder of the test. To avoid disturbing the fresh suspension, a new sample was prepared for each time interval. Tested pastes had a W/C ratio of 0.6.

2.2.2. Water retention experiments

A modified version of the filter paper method (DIN 18 555-7 (DIN (Deutsches Institut für Normung) 2000)) was used to estimate the water retention capacity of the cement paste. (Patural et al. 2010b) validated that the filter paper method is reliable in simulating the actual water migration process that occurs through the interface between a fresh cement paste and a dry porous substrate. A plastic ring (inner diameter 37.4 mm, height 5.7 mm) was placed on top of a stack of creped, fast flow filter paper (Grade 415, VWR, USA) – the schematic is shown in Figure 1. Fresh cement paste was cast into the ring and left there for 20 min. Then, the ring and cement paste were carefully removed from the filter paper. The water retention capacity was calculated from the mass difference of the filter papers before and after the test, as follows:

$$\text{Water retention (\%)} = (1-W_{abs}/W_0) \times 100 \quad (1)$$

where W_{abs} is the water absorbed by the filter paper and W_0 is the mixing water in the cement paste sample. Tested pastes had a W/C ratio of 0.34.

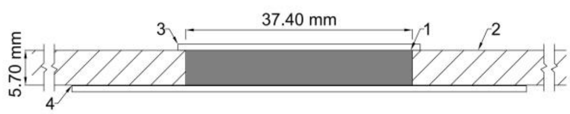

Figure 1. Test setup for determining the water retention of freshly-mixed cement pastes (1. Cement paste, 2. Plastic ring, 3. Cap to prevent evaporation, 4. Filter papers)

2.2.3. Evaporation water loss

A container (height of 47.5 mm, the diameter of 63 mm) was filled with cement paste, placed on a balance, and the mass loss was continuously measured. A commercial fan was positioned approximately 1 m from the setup. The condition was set to 25°C and 10% relative humidity. The mass loss data was smoothed by applying the Savitzky-Golay method of polynomial order 2 and points of window 20 by Origin software (Ghourchian et al. 2018). Tested pastes had a W/C ratio of 0.34, 0.44, and 0.6.

2.3. Rheological measurements

2.3.1. Apparent viscosity and yield stress of cement pastes

Shear rheological tests were performed in a stress-controlled rotational rheometer (HAAKE MARS III, Thermo Fisher Scientific, USA) with a 4-blade vane geometry set at a constant temperature of 25°C. The dimensions were as follows: vane diameter 22 mm, outer cup diameter 26.4 mm, and depth 16 mm. The surface of the outer cylinder was covered with 150-grit adhesive sandpaper to prevent slip.

As fresh cement pastes are thixotropic, it was necessary to pre-shear the pastes to ensure that all samples were at a reproducible reference state (i.e. equilibrium) at the start of each test. To obtain the static yield stress, the stress growth protocol was performed, where deformation was applied at a constant shear rate of 0.1 1/s. The shear stress progressively develops to a maximum value and then decays to an equilibrium value. The static yield stress is defined as the peak shear stress value (Liddel and Boger 1996). As this method is destructive, we prepared a new sample for each yield stress measurement. And the equilibrium value obtained during the pre-shear was taken to be the apparent viscosity. Tested pastes had a W/C ratio of 0.34 and 0.6.

2.3.2. Interstitial solution viscosity

The cement paste pore solution was extracted using a centrifugation approach. Within 10 min after initial cement water contact, prepared cement paste was loaded into vials (36 mL paste in 1.5 mL vial) and centrifuged for 5 min at 4650 rpm. Then, the supernatant was collected, transferred to new vials, then centrifuged again for 5 min at 14500 rpm. The apparent viscosity of the final interstitial solution was tested by a rheometer with a parallel plate setup (diameter 17.5 mm). A logarithmic, increasing shear rate ramp from 1 1/s to 100 1/s was applied over 1000 s. Although a relatively long testing time was applied, inertial effects on the measured viscosity at low shear rates cannot be eliminated in the case of low viscosity polymer solutions (Figure 2) (Poinot et al. 2014). Theoretically, the shear rate does not have any effect if the solution behaves as a Newtonian fluid. At high diutan gum dosages, the viscosity value starts to depend on the shear rate as shear thinning occurs. In our case, at a relatively high dosage of 4%, the interstitial solution viscosity decays to equilibrium at 100 1/s. Therefore 100 1/s was selected to obtain the apparent viscosity of the studied polymer solution.

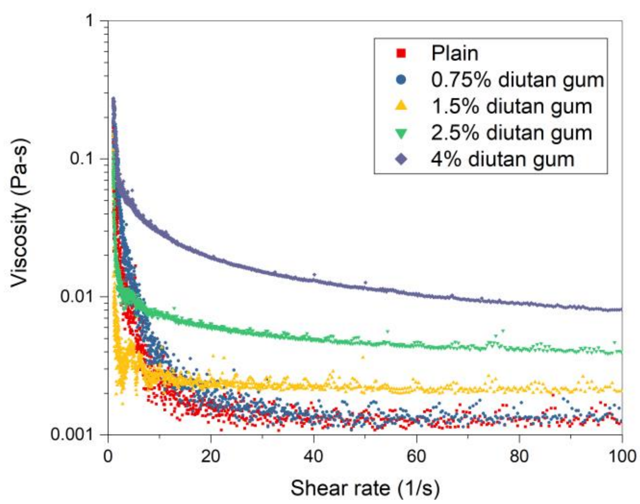

Figure 2. The representative viscosity of diutan gum in solution for various dosages in the polymer as a function of the shear rate. W/C=0.34.

In all the tests, at least three samples per mixture were tested, and the average was taken to be the representative value. Error bars are included in all plots.

3. Results and Discussion

3.1. Bleeding and rheological properties (W/C=0.6)

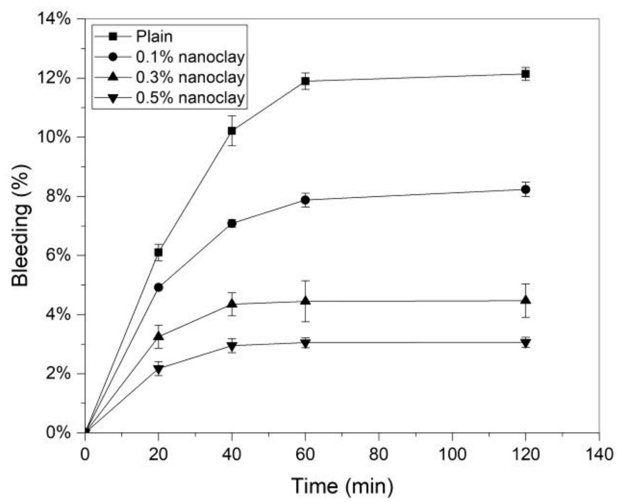

Figure 3. Bleeding behavior with different nanoclay addition. W/C=0.6.

Bleeding evolution was monitored for fresh cement pastes modified with different additions of nanoclay and diutan gum. Results of bleeding were correlated with those of static yield stress. Bleeding water accumulates either through progressive consolidation of the solid skeleton, termed “normal bleeding,” or through the formation of channels, which is usually characterized by a sudden increase in bleeding rate leading to a convex-shaped bleeding-time curve, termed “channeled bleeding” (Tan et al. 1987).

As shown in Figure 3, the plain cement paste and nanoclay modified cement paste shared similar bleeding features as normal bleeding – the bleeding rate is initially constant, followed by a period of diminishing rate before reaching equilibrium. In this case, bleeding can be considered as the process of self-weight consolidation (Tan et al. 1987). The permeability of cement pastes can be derived from the bleeding rate during the constant rate period utilizing Darcy's law:

$$K = Q\, \mu_0 / A g \Delta\rho \quad (2)$$

where K is the permeability of cement paste, Q is the water accumulation rate on the sample surface, A is the cross section of the test tube, μ_0 is the viscosity of the interstitial fluid, $\Delta\rho$ is the density difference between the particles and the liquid, and g is gravitational acceleration. Please note that this equation assumes that the inter-particle forces and other physical-chemical forces are independent of sample depth. As shown in Figure 4, the nanoclay does not have any notable effect on the viscosity of the interstitial fluid. Therefore rate of bleeding depends only on the permeability of the cement paste.

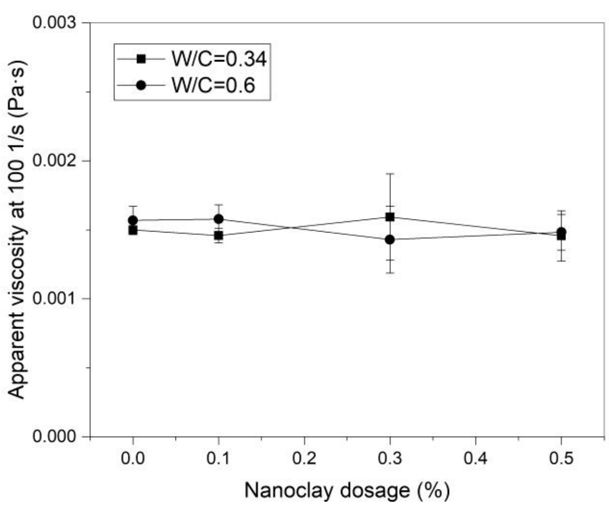

Figure 4. Effect of nanoclay on apparent viscosity of the interstitial solution.

The calculated permeability is shown in Figure 5. (Ferron et al. 2013; Tregger et al. 2010) suggested nanoclay can increase flocculation strength and floc size, which may be attributed to the highly charged particle behavior. The nanoclay carries a negative charge on the faces and a positive charge on the ends (Cao et al. 1996). Nanoclays tend to associate with each other by electrical attraction between positively charged edges and negatively charged surfaces, or absorb on oppositely charged surfaces of cement particles (i.e. C_3S is positively charged in cement suspensions (Zingg et al. 2008)). Also, the fine size and high specific surface area of nanoparticles can provide more contact points and make the suspension structure more interconnected. The resultant structure has higher particle interactions (number and intensity), thereby lowering the permeability (Figure 5). This also leads to an increase in static yield stress, as shown in Figure 6, which is in agreement with previous work (Ma et al. 2018b; Qian and Kawashima 2016). To add, clays have been found to refine the microstructure of hardened cement-based systems, as well (Fan et al. 2014; Ma et al. 2018a).

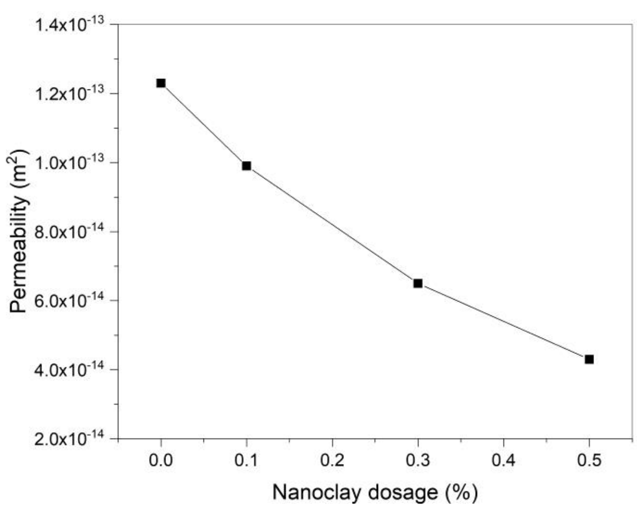

Figure 5. Permeability of cement pastes in bleeding test as a function of nanoclay dosage. W/C=0.6.

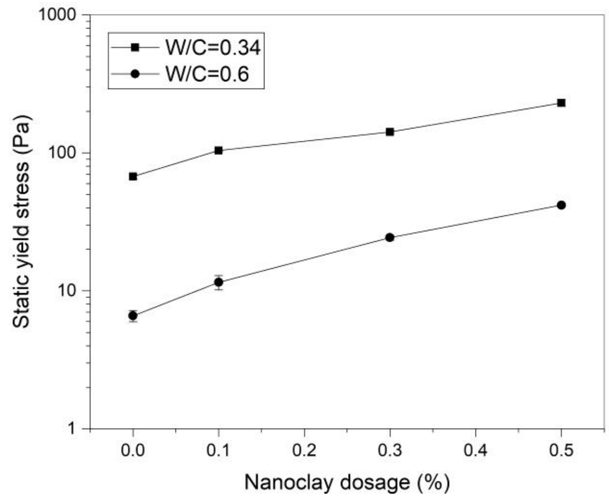

Figure 6. The static yield stress of cement pastes as a function of nanoclay dosage.

In addition to slowing the rate of bleeding, nanoclay addition caused the pastes to reach equilibrium earlier, i.e., 0.5% nanoclay paste reached equilibrium approx. 20 min earlier than plain cement (Figure 3). Bleeding stops when local gravitational forces due to the density difference between cement and water are compensated by the particle interactions, which increases with the local solid volume fraction. Due to its high specific surface area and surface charges, nanoclays induce stronger particle interactions, increase rate of thixotropic rebuilding, and introduce seeding effects, all of which will reduce the difference between local gravitational forces and particle interactions (Kawashima et al. 2013b; Ma et al. 2016).

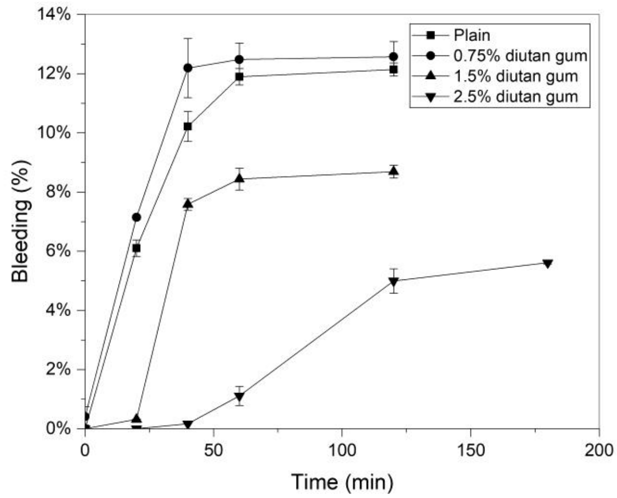

Figure 7. Bleeding behavior with different diutan gum dosages. W/C=0.6.

As shown in Figure 7, in contrast to the monotonic decrease observed with the addition of nanoclay (Figure 3), the diutan gum exhibited a more complex behavior. At a small addition (0.75%), the equilibrium bleeding level increased slightly. Beyond a critical concentration, the addition of diutan gum started to alleviate bleeding until there was no visible bleeding at 4% dosage (not plotted). At concentrations of 0 and 0.75%, the bleeding can be considered as "normal bleeding." At concentrations of 1.5% and 2.5% the bleeding initially progressed at a constant bleeding rate before a sudden increase occurred, after which equilibrium was eventually reached, resulting in a convex bleeding-time curve. This marks channel formation in the cement paste (Loh et al. 1998; Massoussi et al. 2017). During bleeding, the interstitial solution flows upward and induces a viscous drag force on the cement particles. (Massoussi et al. 2017) suggested the viscous drag force causes a progressive local reorganization of the cement paste system. This reorganization leads to the formation of preferred water extraction channels. Research exploring the polysaccharide effect on interstitial solution viscosity suggests the existence of an "overlapping concentration" (Brumaud et al. 2013; Bülichen et al. 2012; Poinot et al. 2014). Below the overlapping concentration, individual polymer molecules exist in pore solutions as isolated coils. Above the overlapping concentration, an exponential rise in viscosity is found as the coils begin to come into contact with one another. This is observed in Figure 8, which shows the viscosity of the interstitial solution of pastes modified with diutan gum. Here, the overlapping concentration is between 0.75% and 1.5%, above which the viscosity increases significantly.

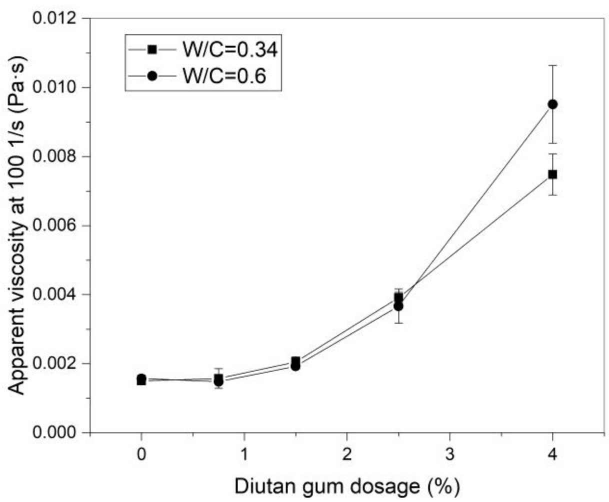

Figure 8. Effect of diutan gum on apparent viscosity of interstitial solution.

The permeability of diutan gum can be calculated by utilizing the bleeding rate during the constant bleeding period. The permeability values are plotted in Figure 9.

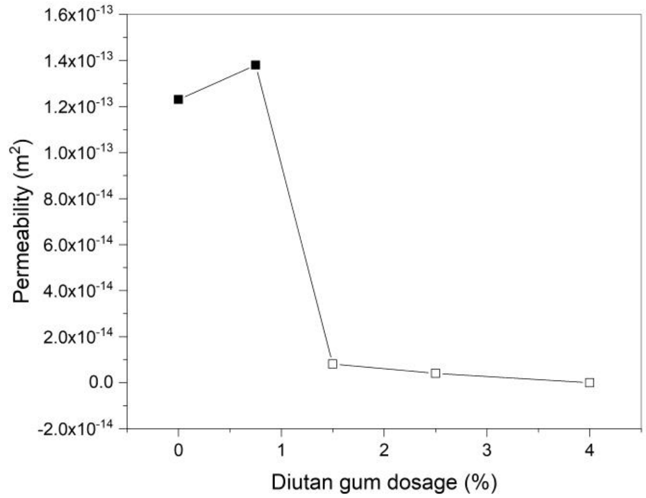

Figure 9. Permeability of cement pastes in bleeding test as a function of diutan gum dosage. As the interstitial solutions start to show shear thinning behaviors at high diutan gum dosages, the permeability can only be estimated approximately by equilibrium viscosity value as marked by open symbols.

W/C=0.6.

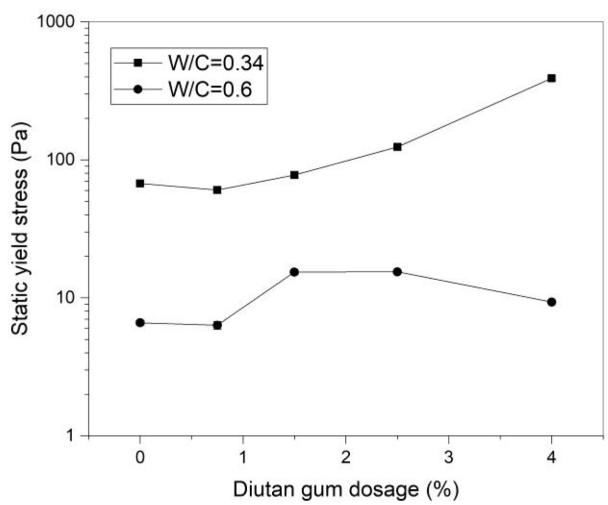

Figure 10. The static yield stress of cement pastes as a function of diutan gum dosage.

Below the overlapping concentration, the permeability increased from 1.23×10^{-13} m^2 to 1.38×10^{-13} m^2 and static yield stress decreased from 6.6 Pa to 6.33 Pa with 0.75% diutan gum addition compared to plain cement paste. This indicates less particle interaction in the structure of the cement paste (number and intensity) with isolated coils existing in the pore solution.

Above the overlapping concentration, at a concentration of 1.5%, the static yield stress increased and the permeability of the cement paste decreased dramatically due to interpenetration and entanglement of the polymer coils. As the concentration was increased further, the addition of diutan gum led to differing effects – a decrease of static yield stress with decrease in permeability. At 4%, the decrease in static yield stress was even more pronounced and there was no apparent bleeding. Thus, the absence of bleeding cannot be attributed to increased colloidal interparticle forces to resist gravity. Besides, the high interstitial solution viscosity can only slow down the bleeding rate according to Darcy's law, not prevent it (assuming before set). There is another key factor that is responsible for the absence of bleeding. (Marliere et al. 2012; Pierre et al. 2015) reported that the polysaccharide aggregates that form above the overlapping concentration could induce jamming and obstruct flow through the cement paste suspension. The flow can be fully stopped if the concentration of polymer aggregates reaches a critical level (Marliere et al. 2012; Pierre et al. 2015). Thus, the absence of bleeding may be attributed to diutan gum aggregates, which block the water flow path completely.

3.2. Water retention and rheological properties (W/C=0.34)

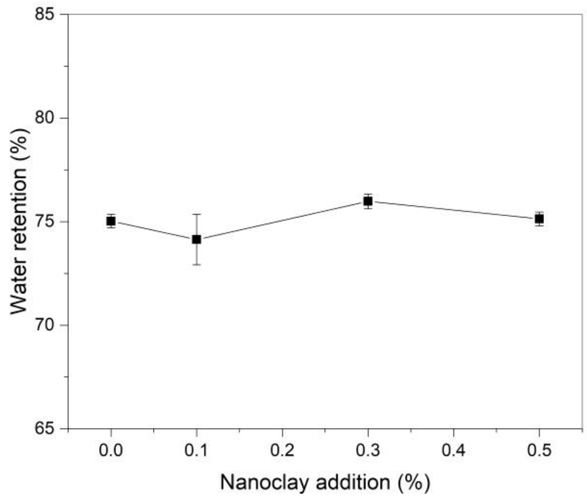

Figure 11. Water retention as a function of nanoclays dosage. Water-cement ratio is 0.34.

The water retention of fresh cement pastes modified with different additions of nanoclay and diutan gum was monitored. Results of water retention are correlated with those of paste and interstitial solution viscosity. As clays have high water sorption capacity, they have been used as absorbents for grease, oil, water, and chemicals since the 1930s (Galan 1996). The characteristic structure of nanoclay provides a significant amount of pore space and permits the absorption of water and other organic materials both on the exterior surface and also in the open channels of the nanoclay crystals (Ginez 1999). At 0.5% addition, assuming a nanoclay water sorption capacity of 200% by mass, from (Kawashima et al. 2012), the water retention should be approx. 3% higher than that of plain cement paste. However, as shown in Figure 11, water retention is independent of nanoclay dosage. A potential explanation is that the water sorption capacity in (Kawashima et al. 2012) was measured using plain water. When incorporated in cement pastes, as in the present study, the ions in the interstitial solution could modify the surface properties of the nanoclay (Xu and Wang 2012), resulting in the deviation of the water sorption capacity.

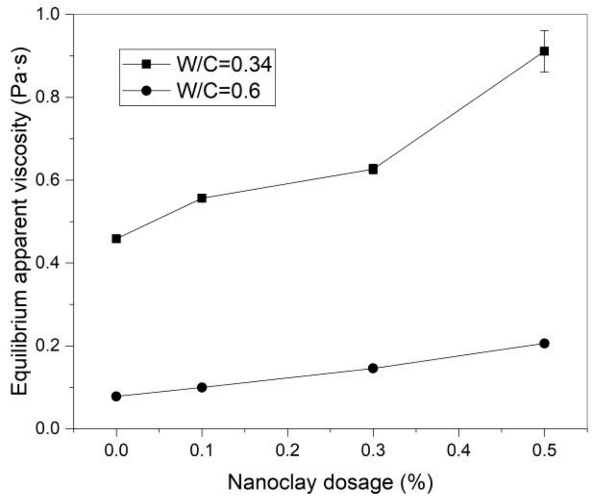

Figure 12. Equilibrium apparent viscosity of different nanoclay dosages under pre-shearing.

The relationship between the rheological properties of cementitious materials and their capacity to retain water has been widely studied (Patural et al. 2010a). Water retention capacity of cement-based materials is commonly explained through mortar viscosity (Ohama 1998; Patural et al. 2010a). By comparing apparent viscosity (Figure 12) and water retention (Figure 11) of nanoclay modified cement pastes, the two parameters do not have the same tendency – apparent viscosity increases while water retention stays the same with nanoclay addition. However, water retention and viscosity of the interstitial solution (see Figure 4) have the same tendency, where neither parameter changes with nanoclay addition.

Although the nanoclay decreases the interstitial fluid mobility in the cement sample, as discussed in section 0, it does not affect the water transport in water retention tests, as shown in Figure 11. In both tests, water moves through the porous matrix of the cement paste in response to a gradient of pressure: local gravity forces induced by the density difference between cement and water in the bleeding test and suction force introduced by the filter paper in the water retention test. However, Darcy's law cannot be applied to the water retention results because the paste undergoes drying (approx. 25% of water is pulled from the cement paste by the filter paper) and Darcy's law requires the paste to be saturated. In this case, the influence of permeability on water loss is complex and needs further investigation.

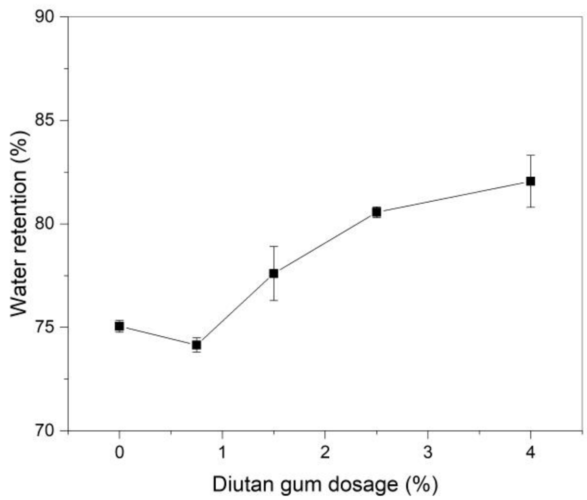

Figure 13. Water retention as a function of diutan gum dosage. Water-cement ratio is 0.34.

Like nanoclay, results clearly show that the water retention (Figure 13) and viscosity (Figure 14) of cement pastes with diutan gum do not show similar tendencies. Therefore paste viscosity is insufficient to explain water retention. Instead, some studies have shown that increase in interstitial solution viscosity correlated well with increase in water retention (Skaggs et al. 1994). This is consistent with what we observed in pastes with both nanoclay and diutan gum addition (Figure 8 and Figure *13*, respectively). Moreover, some studies highlighted the formation of polymer aggregates as the origin of higher interstitial solution viscosity and higher water retention (Marliere et al. 2012; Poinot et al. 2014). To better understand the behavior of diutan gum in cement mixes, we examined the rheological results with different diutan gum concentration.

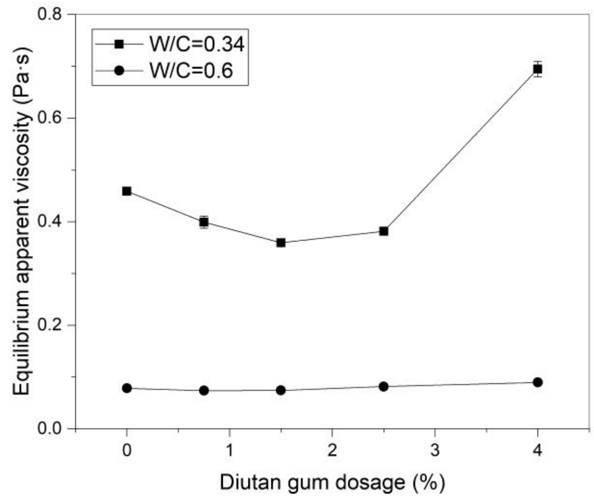

Figure 14. Equilibrium apparent viscosity of different diutan gum dosage under pre-shearing.

Below the overlapping concentration, there was a decrease in equilibrium apparent viscosity, as shown in Figure 14. The lower final equilibrium apparent viscosity may be due to the alignment of polymer molecules. However, a sharp increase in the equilibrium viscosity occurs at 4% addition. As discussed previously, higher polymer additions led to increased interstitial solution viscosity (Figure 8), indicating that polymer aggregates form at these concentrations (Brumaud et al. 2013; Bülichen et al. 2012; Marliere et al. 2012; Pierre et al. 2015). It is hypothesized that the polymer aggregates existing in interstitial solutions may bridge with cement particles to form a strong polymer-cement network that is difficult to break down by shearing, resulting in an increase in apparent viscosity (Figure 14) and static yield stress (Figure 10).

In comparing W/C ratio 0.34 and 0.6, if we look at the static yield stress results, the addition of diutan gum had differing effects: a remarkable increase with W/C ratio 0.34 and a significant drop with W/C ratio 0.6. As mentioned above, the former may be attributed to the formation of a strong polymer-cement network, which cannot be broken down under applied shear. In the latter case, as the system is more diluted, the diutan gum aggregates may form but are not strong enough to resist the shearing. Furthermore, the formed aggregates can increase the distance between cement particles, which will lead to a decay of colloidal force.

3.2. Evaporation water loss (W/C=0.34 and 0.6)

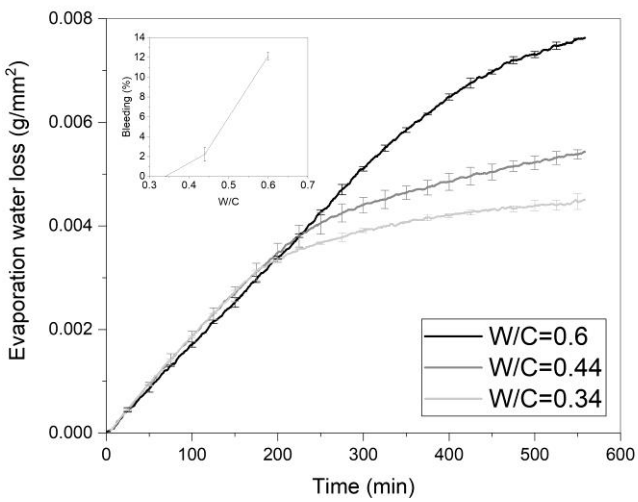

Figure 15. Specific mass change with different W/C ratios.

The effects of W/C ratio and the addition of nanoclay and diutan gum on the rate of evaporation of fresh cement pastes were investigated. Lura et al. (Lura et al. 2007) explain the mechanisms governing the drying behavior of cementitious materials utilizing the drying model of gels presented by (Scherer 1990). First, there is evaporation of accumulated bleed water, where the rate of evaporation is the same as that of bulk water. The second phase is a constant rate period where air-liquid menisci and capillary pressure develop in the top layers and compress the solid skeleton, resulting in the pore fluid surfacing and evaporating. In the final phase, the capillary pressure can no longer compress the solid skeleton and water is drawn from the inside of the specimen. The evaporation rate decreases significantly.

Figure 15 shows the effect of W/C ratio on evaporation water loss. Immediately after placement, at W/C=0.44 and 0.6 water accumulated on top of the sample because the bleeding rate was faster than the evaporation rate (shown in the inset in Figure 15). Thus, after the sample was exposed to air flow, the rate of water loss from the cement paste was close to the rate of free evaporation of water. Once the bleed water dried out (for example, the sample dried out at around 190 min at W/C=0.6), water loss continued at a constant rate as water was pushed to the surface and the sample experienced compression due to the formation of air-liquid menisci. The rate of constant evaporation period was independent of the W/C ratio, and the bleed water did not affect the evaporation rate. However, the lower W/C ratio shortened the duration of the constant rate period. One possible explanation is that a higher W/C ratio causes a higher degree of dilution of cement in the suspension, which may result in a lower rate of hydration and reduced/retarded heat of cement hydration in early ages (Hu et al. 2014). This test is insufficient to fully understand the role of admixtures on evaporation loss, and thus motivates further study implementing techniques, e.g. neutron diffraction, to track water movement.

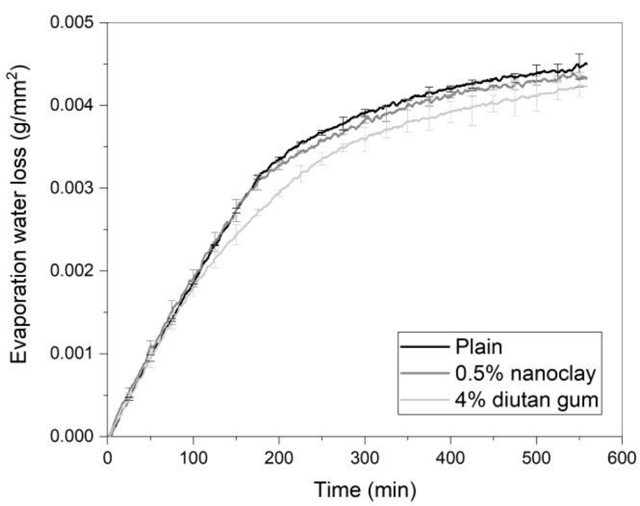

Figure 16. Evaporation with nanoclay and diutan gum. W/C=0.34.

As shown in Figure 16, the nanoclay did not have a notable influence on evaporation water loss at W/C = 0.34. From the above results and analysis (section 0), the nanoclay provides more particle interactions (number and intensity), higher flocculation strength and more contact points. However, due to the relatively high pressure gradient applied to the samples, these interactions do not resist water loss due to evaporation. The diutan gum sample had the same evaporation rate as the plain cement in the first hour. But after that, it showed a faster deviation from the linear evaporation period and went on to exhibit a lower evaporation rate. (Lin and Huang 2010) demonstrates the formation of fibrillose films on the surface of evaporation samples. The rheological results indicated the formation of a strong polymer-cement network, which may at least partially explain the reduction in evaporation rate. Similar trends were seen at W/C = 0.6.

The absence of bleeding water with both nanoclay or diutan gum addition did not curb water loss due to evaporation. In addition, considering the retarding effect of diutan gum on hydration (Ma et al. 2018b), it would have longer evaporation water loss time before setting. Therefore for practical purposes, neither nanoclay nor diutan gum provided resistance to plastic shrinkage. Therefore other methods are needed for mitigation in 3D concrete printing, e.g., curing agents.

Conclusions

This study evaluated the effect of attapulgite/palygorskite clay and diutan gum on the rheological and water transport properties of cement pastes. The key findings are as follows:

1. A monotonic decrease in bleeding was observed with the addition of nanoclay. Cement paste with nanoclay has higher particle interactions, thereby lowering permeability and increasing static yield stress.

2. Below a critical concentration, bleeding increased with increasing dosage of diutan gum. Above a critical level, the cement system exhibited a decrease in bleeding. The addition of diutan gum led to differing effects on yield stress and permeability, which marks the formation of diutan gum aggregates that could block the water flow path and mitigate bleeding.
3. Within the range studied, water retention was independent of nanoclay addition. Results of water retention correlated well with those of interstitial solution viscosity. Diutan gum results highlighted the formation of polymer aggregates as the origin of higher interstitial solution viscosity and higher water retention capacity.
4. The rate of constant evaporation period was independent of W/C ratio, and bleed water was not found to affect evaporation rate.
5. The nanoclay did not have a notable influence on evaporation water loss. Although diutan gum showed slightly lower evaporation rates, in practical terms neither nanoclay nor diutan gum provided resistance to plastic shrinkage. Therefore, other methods will be needed to ensure proper curing for 3D concrete printing, e.g., curing agents.

Acknowledgements

The authors would like to acknowledge the Thornton Tomasetti Student Innovation Fellowship and National Science Foundation (NSF 1653419) for financial support, and technical support by the staff of Columbia University's Carleton Laboratory.

References

"ACTI-GEL® 208 - Acti-Gel." (n.d.). <https://acti-gel.com/acti-gel/> (Apr. 24, 2018).

Brumaud, C., Bessaies-Bey, H., Mohler, C., Baumann, R., Schmitz, M., Radler, M., and Roussel, N. (2013). "Cellulose ethers and water retention." *Cement and Concrete Research*, 53, 176–184.

Bülichen, D., Kainz, J., and Plank, J. (2012). "Working mechanism of methyl hydroxyethyl cellulose (MHEC) as water retention agent." *Cement and Concrete Research*, 42, 953–959.

Cao, E., Bryant, R., and Williams, D. J. A. (1996). "Electrochemical Properties of Na–Attapulgite." *Journal of Colloid and Interface Science*, 179(1), 143–150.

Desbrieres, J. (1993). "Cement cake properties in static filtration. Influence of polymeric additives on cement filter cake permeability." *Cement and Concrete Research*, Pergamon, 23(2), 347–358.

DIN (Deutsches Institut für Normung). (2000). "Testing of mortars containing mineral binders; determination of water retentivity of freshly mixed mortar by the filter plate method." *DIN 18555-7*.

Fan, Y., Zhang, S., Kawashima, S., and Shah, S. P. (2014). "Influence of kaolinite clay on the chloride diffusion property of cement-based materials." *Cement and Concrete Composites*, 45, 117–124.

Ferron, R. D., Shah, S., Fuente, E., and Negro, C. (2013). "Aggregation and breakage kinetics of fresh cement paste." *Cement and Concrete Research*, 50, 1–10.

Galan, E. (1996). "Properties and Applications of Palygorskite-Sepiolite Clays." *Clay Minerals*, 31(4), 443–453.

Ghourchian, S., Wyrzykowski, M., Baquerizo, L., and Lura, P. (2018). "Susceptibility of Portland cement and blended cement concretes to plastic shrinkage cracking." *Cement and Concrete Composites*, 85, 44–55.

Ghourchian, S., Wyrzykowski, M., and Lura, P. (2016). "The bleeding test: A simple method for obtaining the permeability and bulk modulus of fresh concrete." *Cement and Concrete Research*, 89, 249–256.

Ginez, A. (1999). "Attapulgite as a Suspension Control Agent and Rheology Modifier in Flowables." *Pesticide Formulations and Application Systems: Global Pest Control Formulations for the Next Millennium: Nineteenth Volume*, ASTM International, 108-108–10.

Hu, J., Ge, Z., and Wang, K. (2014). “Influence of cement fineness and water-to-cement ratio on mortar early-age heat of hydration and set times.” *Construction and Building Materials*, Elsevier, 50, 657–663.

Kawashima, S., Chaouche, M., Corr, D. J., and Shah, S. P. (2013a). “Rate of thixotropic rebuilding of cement pastes modified with highly purified attapulgite clays.” *Cement and Concrete Research*, 53, 112–118.

Kawashima, S., Hou, P., Corr, D. J., and Shah, S. P. (2013b). “Modification of cement-based materials with nanoparticles.” *Cement and Concrete Composites*, 36, 8–15.

Kawashima, S., Kim, J. H., Corr, D. J., and Shah, S. P. (2012). “Study of the mechanisms underlying the fresh-state response of cementitious materials modified with nanoclays.” *Construction and Building Materials*, 36, 749–757.

Kazemian, A., Yuan, X., Cochran, E., and Khoshnevis, B. (2017). “Cementitious materials for construction-scale 3D printing: Laboratory testing of fresh printing mixture.” *Construction and Building Materials*, Elsevier, 145, 639–647.

Khayat, K. H. (1998). “Viscosity-enhancing admixtures for cement-based materials — An overview.” *Cement and Concrete Composites*, Elsevier, 20(2–3), 171–188.

Khoshnevis, B. (2004). “Automated construction by contour crafting—related robotics and information technologies.” *Automation in Construction*, 13(1), 5–19.

Kim, J. H., Beacraft, M., and Shah, S. P. (2010). “Effect of mineral admixtures on formwork pressure of self-consolidating concrete.” *Cement and Concrete Composites*, 32(9), 665–671.

Liddel, P. V., and Boger, D. V. (1996). “Yield stress measurements with the vane.” *Journal of Non-Newtonian Fluid Mechanics*, 63(2–3), 235–261.

Lin, S.-T., and Huang, R. (2010). “Effect of viscosity modifying agent on plastic shrinkage cracking of cementitious composites." *Materials and Structures*, 43(5), 651–664.

Lloret, E., Shahab, A. R., Linus, M., Flatt, R. J., Gramazio, F., Kohler, M., and Langenberg, S. (2015). "Complex concrete structures: Merging existing casting techniques with digital fabrication." *CAD Computer Aided Design*, 60, 40–49.

Loh, C.-K., Tan, T.-S., Yong, T.-S., and Wee, T.-H. (1998). "An experimental study on bleeding and channelling of cement paste and mortar." *Advances in Cement Research*, 10(1), 1–16.

Lura, P., Pease, B., Mazzotta, G. B., Rajabipour, F., and Weiss, J. (2007). "Influence of Shrinkage-Reducing Admixtures on Development of Plastic Shrinkage Cracks." *ACI Materials Journal*, 104(2), 187–194.

Ma, S., Qian, Y., and Kawashima, S. (2018a). "Performance-based study on the rheological and hardened properties of blended cement mortars incorporating palygorskite clays and carbon nanotubes." *Construction and Building Materials*, 171, 663–671.

Ma, S., Qian, Y., and Kawashima, S. (2018b). "Experimental and modeling study on the non-linear structural build-up of fresh cement pastes incorporating viscosity modifying admixtures." *Cement and Concrete Research*, 108, 1–9.

Ma, S., Yu, T., Wang, Y., Chaouche, M., and Kawashima, S. (2016). "Phase Evolution of Oil Well Cements with Nano-additive at Elevated Temperature/Pressure." *ACI Materials Journal*, 113(5).

Marliere, C., Mabrouk, E., Lamblet, M., and Coussot, P. (2012). "How water retention in porous media with cellulose ethers works." *Cement and Concrete Research*, 42, 1501–1512.

Massoussi, N., Keita, E., and Roussel, N. (2017). "The heterogeneous nature of bleeding in cement pastes." *Cement and Concrete Research*, 95, 108–116.

Mehta, P., and Monteiro, P. J. M. (2006). *Concrete: Microstructure, Properties, and Materials*. McGraw-Hill Education.

Murray, H. H. (1991). “Overview — clay mineral applications.” *Applied Clay Science*, 5(5–6), 379–395.

Ohama, Y. (1998). “Polymer-based admixtures.” *Cement and Concrete Composites*, Elsevier, 20(2–3), 189–212.

Patural, L., Marchal, P., Govin, A., Grosseau, P., Ruot, B., and Devès, O. (2010a). “Cellulose ethers influence on water retention and consistency in cement-based mortars.” *Cement and Concrete Research*, 41, 46–55.

Patural, L., Porion, P., Van Damme, H., Govin, A., Grosseau, P., Ruot, B., and Devès, O. (2010b). “A pulsed field gradient and NMR imaging investigations of the water retention mechanism by cellulose ethers in mortars.” *Cement and Concrete Research*, Pergamon, 40(9), 1378–1385.

Pei, R., Liu, J., and Wang, S. (2015). “Use of bacterial cell walls as a viscosity-modifying admixture of concrete.” *Cement and Concrete Composites*, Elsevier, 55, 186–195.

Perrot, A., Lecompte, T., Khelifi, H., Brumaud, C., Hot, J., and Roussel, N. (2012). “Yield stress and bleeding of fresh cement pastes.” *Cement and Concrete Research*, 42(7), 937–944.

Pierre, A., Perrot, A., Picandet, V., and Guevel, Y. (2015). “Cellulose ethers and cement paste permeability.” *Cement and Concrete Research*, 72, 117–127.

Plank, J. (2004). “Applications of biopolymers and other biotechnological products in building materials.” *Applied Microbiology and Biotechnology*, Springer-Verlag, 66(1), 1–9.

Poinot, T., Govin, A., and Grosseau, P. (2014). “Importance of coil-overlapping for the effectiveness of hydroxypropylguars as water retention agent in cement-based mortars.” *Cement and Concrete Research*, 56, 61–68.

Qian, Y., and Kawashima, S. (2016). “Use of creep recovery protocol to measure static yield stress and structural rebuilding of fresh cement pastes.” *Cement and Concrete Research*, 90, 73–79.

Quanji, Z., Lomboy, G. R., and Wang, K. (2014). “Influence of nano-sized highly purified magnesium alumino silicate clay on thixotropic behavior of fresh cement pastes.” *Construction and Building Materials*, 69, 295–300.

Sanjayan, J. G., Nematollahi, B., Xia, M., and Marchment, T. (2018). “Effect of surface moisture on inter-layer strength of 3D printed concrete.” *Construction and Building Materials*, 172, 468–475.

Scherer, G. W. (1990). “Theory of Drying.” *Journal of the American Ceramic Society*, Blackwell Publishing Ltd, 73(1), 3–14.

Skaggs, C. B., Rakitsky, W. G., and Whitaker, S. F. (1994). “Applications of Rheological Modifiers and Superplasticizers in Cementitious Systems.” *Special Publication*, 148, 189–208.

Tan, T. S., Wee, T. H., Tan, S. A., Tam, C. T., and Lee, S. L. (1987). “A consolidation model for bleeding of cement paste.” *Advances in Cement Research*, 1(1), 18–26.

Tregger, N. A., Pakula, M. E., and Shah, S. P. (2010). “Influence of clays on the rheology of cement pastes.” *Cement and Concrete Research*, 40(3), 384–391.

Voigt, T., Mbele, J.-J., Wang, K., and Shah, S. P. (2010). “Using Fly Ash, Clay, and Fibers for Simultaneous Improvement of Concrete Green Strength and Consolidatability for Slip-Form Pavement.” *Journal of Materials in Civil Engineering*, 22(2), 196–206.

Xu, J., and Wang, A. (2012). “Electrokinetic and Colloidal Properties of Homogenized and Unhomogenized Palygorskite in the Presence of Electrolytes.” *Journal of Chemical & Engineering Data*, 57(5), 1586–1593.

Zingg, A., Winnefeld, F., Holzer, L., Pakusch, J., Becker, S., and Gauckler, L. (2008). “Adsorption of polyelectrolytes and its influence on the rheology, zeta potential, and microstructure of various cement and hydrate phases.” *Journal of Colloid and Interface Science*, 323(2), 301–312.

List of Table

Table 1. Chemical composition of Type I Portland Cement.

Chemical Oxide	SiO_2	Al_2O_3	Fe_2O_3	CaO	MgO	SO_3	Loss on ignition
Cement (%)	19.27	4.68	3.51	63	3.21	2.72	2.09

List of Figures